J Nanopart Res (2015) 17:355
DOI 10.1007/s11051-015-3133-z

RESEARCH PAPER

Protein surface labeling reactivity of *N*-hydroxysuccinimide esters conjugated to Fe_3O_4@SiO_2 magnetic nanoparticles

Parisa Pirani · Ujwal S. Patil · Tushar Dattu Apsunde · Mark L. Trudell · Yang Cai · Matthew A. Tarr

Received: 21 April 2015 / Accepted: 23 July 2015 / Published online: 2 September 2015

Abstract The *N*-hydroxysuccinimide (NHS) ester moiety is one of the most widely used amine reactive groups for covalent conjugation of proteins/peptides to other functional targets. In this study, a cleave-analyze approach was developed to quantify NHS ester groups conjugated to silica-coated iron oxide magnetic nanoparticles (Fe_3O_4@SiO_2 MNPs). The fluorophore dansylcadaverine was attached to Fe_3O_4@SiO_2 magnetic nanoparticles (MNPs) via reaction with NHS ester groups, and then released from the MNPs by cleavage of the disulfide bond in the linker between the fluorophore and the MNPs moiety. The fluorophore released from Fe_3O_4@SiO_2 MNPs was fluorometrically measured, and the amount of fluorophore should be equivalent to the quantity of the NHS ester groups on the surface of Fe_3O_4@SiO_2 MNPs that participated in the fluorophore conjugation reaction. Another sensitive and semiquantitative fluorescence microscopic test was also developed to confirm the presence of NHS ester groups on the surface of Fe_3O_4@SiO_2 MNPs. Surface-conjugated NHS ester group measurements were primarily performed on Fe_3O_4@SiO_2 MNPs of 100–150 nm in diameter and also on 20-nm nanoparticles of the same type but prepared by a different method. The efficiency of labeling native proteins by NHS ester-coated Fe_3O_4@SiO_2 MNPs was explored in terms of maximizing the number of MNPs conjugated per BSA molecule or maximizing the number of BSA molecules conjugated per each nanoparticle. Maintaining the amount of fresh NHS ester moieties in the labeling reaction system was essential especially when maximizing the number of MNPs conjugated per protein molecule. The methodology demonstrated in this study can serve as a guide in labeling the exposed portions of proteins by bulky multivalent labeling reagents.

Keywords Surface exposed amine groups · Nanoparticle surface ligand quantification · Protein surface labeling · Magnetic iron oxide nanoparticles

Parisa Pirani and Ujwal S. Patil have contributed equally to this work.

Electronic supplementary material The online version of this article (doi:10.1007/s11051-015-3133-z) contains supplementary material, which is available to authorized users.

P. Pirani · U. S. Patil · T. D. Apsunde · M. L. Trudell · Y. Cai · M. A. Tarr (✉)
Department of Chemistry, University of New Orleans, 2000 Lakeshore Drive, New Orleans, LA 70148, USA
e-mail: mtarr@uno.edu

Y. Cai (✉)
The Research Institute for Children, Children's Hospital, 200 Henry Clay Avenue, New Orleans, LA 70118, USA
e-mail: ycai@chnola-research.org

Introduction

Iron oxide-based magnetic nanoparticles have found a wide range of applications largely due to robust superparamagnetization (Gupta and Gupta 2005; He

et al. 2014) and simple preparation of this type of nanomaterials. Superparamagnetism allows for easy magnetic separation of ligands covalently or noncovalently attached to the iron oxide nanoparticles, while the nanoparticle–ligand complex could still be well dispersed in solution in the absence of a magnetic field. Preparation of a magnetic iron oxide core is quite simple, and the magnetic core can also be coated by silica, polyethylene glycol, dextran, and other functional groups to improve the aqueous compatibility (Turcheniuk et al. 2013) of the coated MNPs. A nonporous layer of silica can protect the iron oxide magnetic nanoparticle core from oxidation and from unnecessary chelation between ferrous/ferric ions and ligands. The size and superparamagnetic properties of Fe_3O_4@SiO_2 MNPs are tunable (Kolhatkar et al. 2013) to accommodate a variety of biomedical applications (Malvindi et al. 2011; Larumbe et al. 2012; Chiriaco et al. 2013). Functional groups, such as amine, thiol, and carboxylic acid, can be immobilized on the surface of MNPs before further conjugation of other ligands (Sapsford et al. 2013). The ligands present on the surface of MNPs are also important to define the application of this type of nanomaterial (Verma and Stellacci 2010). For instance, positively charged, aminodextran-coated Fe_3O_4 MNPs showed improved uptake in Hela cells compared to neutral, dextran-coated, and negative dimercaptosuccinic MNPs (Villanueva et al. 2009).

Determining the amount of reactive functional groups (amine, thiol, carboxyl, etc.) on the surface of nanomaterials is critical for further conjugation of biomolecules to the surface. Compared to numerous efforts on the syntheses of biocompatible nanoparticles, much less attention has been paid to quantification of intermediate functional groups and exposed ligands on the nanomaterials' surface. Some straightforward approaches to quantify ligands on solid surfaces (not necessarily nanomaterials) involve covalent or noncovalent conjugation of a chromophore/fluorophore to the surface functional groups, and quantitation of the conjugated chromophore/fluorophore to determine the equivalent amount of ligands on the solid surfaces (Xing et al. 2007). A few examples of quantifying amine groups on solid surfaces via covalent interaction with chromophore/fluorophore include fluorescamine assay (Chen et al. 2006; Corsi et al. 2003; Kell and Simard 2007) fluorescent Fmoc-CL assay, (Chen and Zhang 2011); (Zhang and Chen 2012) NHS-fluorescein assay (Maus et al. 2009), 4-nitrobenzaldehyde detection by using UV–Vis spectroscopy (Bruce and Sen 2005; Kim et al. 2007; Ghasemi et al. 2007), and bromophenol blue assay (Ghasemi et al. 2007). A carboxyl-modified fluorescent dye (4,4-difluoro-5,7-dimethyl-4-bora-3a,4a-diaza-s-indacene-3-propionic acid) was covalently conjugated to amine groups on a glass slide followed by fluorometric quantification of the fluorophore-conjugated amine groups (Xing and Borguet 2006). Similarly, thiol groups on solid surfaces could be quantified by measuring a yellow-colored product resulting from the covalent binding of Ellman's reagent to the free thiol groups (Bravo-Osuna et al. 2007). Aldehyde groups on a glass slide were quantified by covalent conjugation of this functional group to a hydrazine-modified fluorescent dye (4,4-difluoro-5,7-dimethyl-4-bora-3a,4a-diaza-s-indacene-3-propionic acid, hydrazide) followed by fluorometric measurement (Xing and Borguet 2006). In order to avoid any interference from solid surfaces, fluorophores/chromophores covalently conjugated to solid surfaces can be detached prior to the measurement, and this type of method has been known as the cleave-analyze approach (Liu and Yan 2011). Attaching noncovalently chromophores/fluorophores such as orange II dye (Noel et al. 2011) or coomassie brilliant blue (Bradford assay) (Coussot et al. 2009) to amine groups on solid surfaces has also been used for amine quantification.

Elemental analysis approaches, such as time-of-flight-secondary ion mass spectrometry (ToF–SIMS) (Kim et al. 2005), carbon–hydrogen–nitrogen combustion analysis (van de Waterbeemd et al. 2010), and X-ray photoelectron spectroscopy (XPS) were used to quantify primary amine groups (Noel et al. 2011; Dauginet et al. 2001). Thiol groups on the surface of gold nanoparticles were quantified by means of inductively coupled plasma-mass spectrometry (ICP-MS) (Hinterwirth et al. 2013; Elzey et al. 2012). Yan et al. recently quantified dopamine-anchoring group on the surface of MNPs by means of laser desorption ionization mass spectrometry (LDI-MS) (Yan et al. 2013). These elemental analysis approaches (ToF–SIMS, XPS, ICP-MS, and LDI-MS) usually work better for smaller nanoparticles such as gold nanoparticles with a few gold atoms (Noel et al. 2011). It is also possible to quantify ligands on solid surface by indirect measurement of the side-products in the reactions that

further modify the ligands. For example, the heterobifucntional crosslinkers *N*-(succinimidyl 3-(2-pyridyldithio) propionate (SPDP), and succinimidyl 6-[3′-(2-pyridyldithio)-propionamido] hexanoate (LC-SPDP) react with primary amine groups and quantitatively yield pyridine-2-thione. Spectrophotometric measurement of pyridine-2-thione can be used to quantify the amount of amine groups immobilized on solid surfaces (Schellenberger et al. 2004; Noel et al. 2011; Fang et al. 2009). In an indirect iodine titration that quantified thiol groups on chitosan MNPs, iodine was used to oxidize thiol groups, and the remaining iodine in solution was determined by the brilliant blue color resulting from the starch–iodine complexion (Bravo-Osuna et al. 2007). The amount of thiol groups was calculated by the subtraction of the unconsumed iodine from the initial amount of iodine added. These indirect measurement methods are ligand specific and highly dependent on the ligand modification reaction. The depletion approach that measures the difference between the initial and the final amounts of fluorophore after covalent conjugation to the surface was utilized for quantification of hydroxyl, carboxylic acid, and aldehyde/ketone groups on solid surfaces (Feng et al. 2006); (Dementev et al. 2009; Pellenbarg et al. 2010). Moreover, Fourier transform-infrared (FTIR) absorbance spectroscopy was used for quantitative monitoring of ester carbonyl and aldehyde carbonyl groups in benzimidazole synthesis reaction which was performed on the solid phase (Sun and Yan 1998); and the technique was also applied in relative quantification of carbonyl-containing ligands on the surface of gold nanoparticles (Zhou et al. 2010).

The NHS ester group reacts with primary amine groups to form a covalent bond, and this conjugation chemistry is widely used in the field of biomaterials science because the reaction can proceed under physiological conditions with high specificity. Ligands, such as peptides, proteins, and genetic materials, can be conjugated on the surface of MNPs through NHS ester-amine chemistry. The modified MNPs have found many clinical applications, including magnetic resonance imaging, fluorescence imaging, theranostic agents, detection of biomarkers, cell sorting, and enrichment of protein samples from complex mixtures (Sapsford et al. 2013; Urbanova et al. 2014). Recently in our lab, NHS ester-modified $Fe_3O_4@SiO_2$ MNPs with cleavable disulfide bond linker were developed to label primary amine groups on the solvent-accessible surface of proteins (Patil et al. 2013). Protein labeling was achieved via the reaction between NHS ester moiety and primary amine group under conditions that the native structure of protein was preserved. In order to verify the conjugation of NHS ester moiety to the surface of $Fe_3O_4@SiO_2$ MNPs, it is necessary to develop a more sensitive fluorescence microscopic quantification approach based on covalent attachment of fluorophore dansylcadaverine to MNPs. Through a cleave-analyze approach, dansylcadaverine (Ikari et al. 2011) conjugated to $Fe_3O_4@SiO_2$ MNPs could be more accurately measured in HPLC analyses in order to determine the amount of NHS ester/thiol groups on MNPs surface. Quantification of NHS ester groups on $Fe_3O_4@SiO_2$ MNPs surface provided the basis for investigations on the reactivity of the magnetic nanoparticle reagent in labeling native proteins.

Experimental procedures

All chemical reagents were of reagent grade, obtained from commercial sources and used as received without further purification unless specified otherwise. Details are provided in supporting information. $Fe_3O_4@SiO_2$ nanoparticles were prepared as previously reported (Liu et al 2013; Yu et al. 2004) with minor changes (Supporting Information).

Conjugation of dansylcadaverine to NHS ester-modified $Fe_3O_4@SiO_2$ MNPs

NHS ester-coated $Fe_3O_4@SiO_2$ MNPs (100-nm diameter, 7 mg) or smaller NHS ester-coated $Fe_3O_4@SiO_2$ MNPs (20-nm diameter, 6 mg) were incubated with dansylcadaverine (2 mM, 1 mL in ethanol) in the dark at room temperature for 1 h. The dansylcadaverine-conjugated MNPs were collected by an external magnet and washed repeatedly with dimethyl sulfoxide (DMSO), ethanol, and water (nanopure water produced by a Barnstead Nanopure UV water treatment system, Millipore, Billerica, MA). Dansylcadaverine-modified MNPs were treated with tris(2-carboxyethyl)phosphine (TCEP, 50 mM) solution in water (300 μL) at room temperature for 1 h. The cleaved product (3-mercaptopropanamido dansylcadaverine, 3-MPA-Dansyl) was recovered by repeatedly washing the MNPs and by magnetic separation.

The supernatant and the wash solutions were combined and dried under vacuum. The cleaved 3-MPA-Dansyl samples were dissolved in 20:80 acetonitrile:water (1 mL) prior to HPLC analysis.

Synthesis of 3-MPA-Dansyl

Dansyl cadaverine derivative 3-MPA-Dansyl (3-mercaptopropanamido dansylcadaverine) is not commercially available. Preparation of this standard for quantification is provided in Supporting Information.

HPLC instrumentation and chromatography conditions

An Agilent 1100 HPLC system (Agilent, Santa Clara, CA) equipped with 1100 series quaternary gradient pump, vacuum degasser, and HP 1046A fluorescence detector was used for all measurements. Isocratic elution with a mobile phase of 80 % acetonitrile and 20 % water was used for all measurements. The detector was set at 335 nm for excitation and 530 nm for emission. A GRACE VisionHT^{TM} C18 Classic 5 μm 150 × 4.6 mm column (Grace, Columbia, MD) was used for all analyses at ambient temperature with a flow rate of 0.8 mL/min.

Fluorescence microscopy imaging of dansylcadaverine-modified $Fe_3O_4@SiO_2$ MNPs

NHS ester-modified $Fe_3O_4@SiO_2$ MNPs (100-nm diameter, 1 mg) were incubated at room temperature with 1 mL of 2 mM dansylcadaverine in ethanol for 1 h. The nanoparticles were separated by magnetic field and washed multiple times with DMSO, water, and ethanol. The fluorophore-conjugated magnetic nanoparticles were redispersed in ethanol (1 mL), and small aliquots were transferred to a glass slide and air-dried in the dark prior to fluorescence microscopy imaging. An Olympus IX 71 inverted fluorescence microscope with a high-performance 16-bit resolution, back-illuminated CCD camera (Roper Scientific), and a 100-W Hg lamp as the light source was used for the measurements. The fluorescence images were taken through a 40× microscope objective with numerical aperture (NA) = 0.75. The filter cube of the microscope contained a 450 ± 10-nm bandpass excitation filter, a 505-nm dichroic mirror, and a 515-nm long-pass emission filter.

A program run under MATLAB® (MATLAB 2013) was written for fluorescence intensity integration. The fluorescence intensities of dansylcadaverine-conjugated MNPs in a fluorescence microscope image were calculated in two steps. First, the color image (red, green, blue) was converted to a grayscale image. Second, the intensities of bright spots on this grayscale image were calculated by adding the intensities of pixels together. In the grayscale image, the background pixels were converted to black pixels. Therefore, the background was removed from the intensity integration. The brightness of a pixel was normalized to the scale from 0 to 1. More details of the program can be found in the supporting information.

Measurement of BSA conjugated to $Fe_3O_4@SiO_2$ nanoparticles

Bovine serum albumin (BSA) solution (1 mL of 1 mg/mL) in phosphate-buffered saline (PBS, 10 mM, pH 7.4) was incubated with iodoacetamide (20 mM) in the dark at 37 °C for 1 h, then the mixture was diluted with PBS to 0.5 mg/mL of BSA. Mixing of the NHS ester-modified $Fe_3O4@SiO_2$ (100-nm diameter) MNPs with the BSA solution (0.5 mg/mL in PBS pH 7.4) was performed according to Fig. S7 (Supporting Information). The MNPs were washed several times with water and acetonitrile (70 %). All the washes were combined, centrifuged, dried under vacuum, and redissolved in 10 μL of nanopure water. The unconjugated BSA in the combined washes was quantified by means of a micro-bicinchoninic acid (BCA) assay kit (Thermo Scientific, Rockford, IL) according to the protocol provided by the manufacturer. The amount of BSA conjugated to the MNPs labeling reagent was calculated by subtraction of unconjugated BSA from the initial amount of fresh BSA used for labeling reaction.

Results and discussion

Control of the size and shape of $Fe_3O_4@SiO_2$ MNPs employed in this study was significantly improved compared to that of the $Fe_3O_4@SiO_2$ MNPs in our previous proof of the concept study. (Patil et al. 2013) Even though $Fe_3O_4@SiO_2$ MNPs with irregular shapes showed superparamagnetism, it was difficult to estimate the surface areas of these particles, and

hence the number of intermediate functional groups (e.g., primary amine, thiol) per MNPs surface area. Moreover, the irregular shapes of MNPs might also add steric hindrance to the approaching protein molecules, thus affecting the number of protein molecules that could bind to the MNPs. The size and shape uniformity of larger $Fe_3O_4@SiO_2$ MNPs (100-nm diameter) and smaller $Fe_3O_4@SiO_2$ MNPs (20-nm diameter), as indicated by the TEM images (Fig. 1 and Fig. S2B), facilitated improved characterization of the surface-modified MNPs.

NHS ester-conjugated $Fe_3O_4@SiO_2$ MNPs

The magnetite core of $Fe_3O_4@SiO_2$ MNPs was prepared by a hydrothermal method (Liu et al 2013) (Fig. S1, Supporting Information.). TEM image analysis of $Fe_3O_4@SiO_2$ MNPs confirmed the spherical and uniform nature of the magnetite core with diameters of 80 ± 5 nm. The Stöber method (Lu et al. 2002) was applied for coating the magnetite core with a silica layer to form $Fe_3O_4@SiO_2$ MNPs with 100 ± 10-nm diameters (Fig. 1). Smaller $Fe_3O_4@SiO_2$ MNPs (20-nm diameter) also with improved uniformity in size and shape, were prepared and employed in this study, but the majority of the experiments were performed on larger MNPs. The particles with the smaller magnetite core were prepared by thermal decomposition and coated with silica by means of the reverse microemulsion approach (Cannas et al. 2010). Fig. S2A provides details for their preparation, and Fig. S2B illustrates representative particles (Supporting Information). The smaller $Fe_3O_4@SiO_2$ MNPs (20-nm diameter, Fig.S2B) were nearly uniform and dispersible in water, ethanol, and PBS. The silica coating provided improved aqueous stability as well as protection from oxidation and reduced nonspecific interactions with ligands.

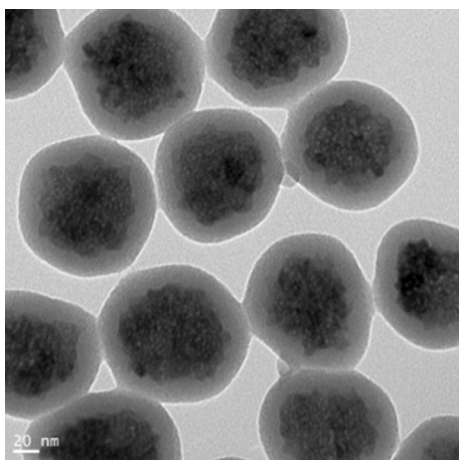

Fig. 1 TEM image of $Fe_3O_4@SiO_2$ (100 nm in diameter) prepared by modified Stöber method. MNPs were uniform in size and shape, and well dispersible in aqueous solvents

The 100- and 20-nm $Fe_3O_4@SiO_2$ MNPs were further functionalized with thiol groups using MPTMS. The theoretical quantity of thiol groups that could be conjugated to the surface of 100-nm $Fe_3O_4@SiO_2$ MNPs was calculated to be about 10^5 per particle, with the estimate based on these parameters: density of MNPs (4.5 g/cm^3), total mass of MNPs (1 mg), bond length of Si–O (171 pm), and bond angle of O-Si–O (109.5°). The total surface area of particles and the estimated surface area required per MPTMS were then used to determine the theoretical number of surface groups after modification. The amount of SPDP for free thiol group conjugation could be estimated based on the theoretical number of thiol groups on MNPs surface; for example, 1 mg of 100-nm $Fe_3O_4@SiO_2$ MNPs should be able to react with 22 μg of SPDP.

Fluorescence-based quantification of active NHS ester groups on the surface of $Fe_3O_4@SiO_2$ MNPs

The fluorophore dansylcadaverine contains a primary amine group similar to that in the side chain of the amino acid lysine, so the fluorophore can also be covalently attached to NHS ester-conjugated $Fe_3O_4@SiO_2$ MNPs via a nucleophilic substitution reaction between the NHS ester and the primary amine. In the structure of dansylcadaverine-conjugated $Fe_3O_4@SiO_2$ MNPs (Fig. S6), a disulfide bond is incorporated in the spacer/linker between the fluorophore moiety and the $Fe_3O_4@SiO_2$ MNPs moiety. Upon reductive cleavage of the disulfide bond in the spacer/linker, the fluorophore moiety can be cleaved from $Fe_3O_4@SiO_2$ MNPs. Whether attached to or released from the $Fe_3O_4@SiO_2$ MNPs, the fluorescent dansylcadaverine moiety should serve as an indicator for quantification of NHS ester groups on the surface of $Fe_3O_4@SiO_2$ MNPs.

Quantification of NHS ester groups by cleave-analyze approach

Upon cleavage of the disulfide bond in the linker between the dansylcadaverine moiety and the $Fe_3O_4@SiO_2$ MNPs (structure in Fig. S3), 3-MPA-Dansyl

was released and analyzed by HPLC with fluorescence detection, which facilitated separation from TCEP, which is reported to affect the fluorescence of various fluorophores (Vaughan et al. 2013). For accurate quantification of dansylcadaverine released from the fluorophore-modified Fe_3O_4@SiO_2 MNPs, the calibration standard, 3-MPA-Dansyl, was synthesized (Fig. S3 Supporting Information) and characterized by fluorescence spectroscopy (Fig. S4), mass spectrometry, and NMR (Supporting Information). The released 3-MPA-Dansyl from MNPs showed the same retention time as that of synthesized 3-MPA-Dansyl calibration standard, but eluted from the HPLC column faster than unmodified dansylcadaverine (Fig. 2).

The number of dansylcadaverine molecules per Fe_3O_4@SiO_2 MNP could be predicted based on the size of the nanoparticle (determined by TEM), density of MNPs (estimated based on the structure of Fe_3O_4@SiO_2, i.e., the size of magnetite core and the thickness of the silica coating layer), and the amount of 3-MPA-Dansyl released from dansylcadaverine-conjugated Fe_3O_4@SiO_2 MNPs. For the smaller Fe_3O_4@SiO_2 MNPs (20-nm diameter, 6 mg), the amount of conjugated dansylcadaverine was determined by HPLC to be 2.4×10^{-7} mol. The number of dansylcadaverine molecules per MNP was calculated based on the following assumptions. The density of 20-nm diameter Fe_3O_4@SiO_2 MNPs was estimated to be 2.5 g/cm^3 according to the density values of Fe_3O_4 (5.17 g/cm^3) and SiO_2 (2.2 g/cm^3) (Simon and Sze 1981). Consequently, 6 mg of these MNP contained approximately 5.62×10^{14} particles, the average number of dansylcadaverine conjugated to one nanoparticle was about 2.6×10^2, and the number of conjugated dansylcadaverine per milligram of 20-nm MNPs was 2.4×10^{16}. Similarly, it can be estimated that for 100-nm Fe_3O_4@SiO_2 MNPs, the average number of dansylcadaverine conjugated to one nanoparticle surface was about 3.4×10^3, and the number of conjugated dansylcadaverine per milligram of 100-nm MNPs that approximately contained 4.27×10^{11} particles, was 1.4×10^{15}. With 1:1 stoichiometry and optimal efficiency, the number of 3-MPA-Dansyl molecules released should be equal to the number of NHS ester groups on the MNP surface. However, the experimentally determined number of NHS ester groups on each 100-nm Fe_3O_4@SiO_2 MNP was less than the theoretical maximum number of thiol groups that could attach to the MNP surface ($\sim 10^5$). The difference could be due to the hydrolysis of NHS ester groups in contact with moisture in the solvent or air between preparation of the particles and binding to the fluorophore. Steric hindrance may also contribute to the observed difference in conjugation efficiency.

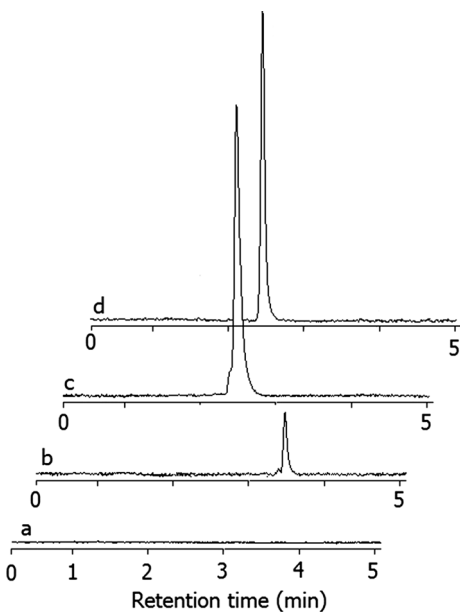

Fig. 2 Chromatogram obtained by HPLC-fluorescence analysis of *a* Control, *b* dansylcadaverine (5 μM) *c* 3-MPA-Dansyl (20 μM), and *d* 3-MPA-Dansyl released from 7 mg of Fe_3O_4@SiO_2 MNPs (100 nm in diameter) upon cleaving the disulfide bond. For all samples, the injection volume was 100 μl. The isocratic elution with mobile phase of 80 % ACN and 20 % H_2O was performed for all samples. The control sample was prepared by reacting thiol-coated MNPs (7 mg) with dansylcadaverine

Semiquantitative fluorescence microscopic characterization of danylcadaverine-modified Fe_3O_4@SiO_2 MNPs

Fluorescence microscopy was used as a rapid and sensitive technique for qualitative and semi-quantitative characterization of active NHS ester groups covalently attached to dansylcadaverine. The green fluorescence of dansylcadaverine-conjugated Fe_3O_4@SiO_2 MNPs was detected by a fluorescence microscope (Fig. 3). Fluorescence microscopic analysis allowed us to develop a quick test to determine the presence of NHS esters on the surface of Fe_3O_4@SiO_2 MNPs. Thiol-coated Fe_3O_4@SiO_2 MNPs were used as a negative control (i.e., no dansylcadaverine) under the

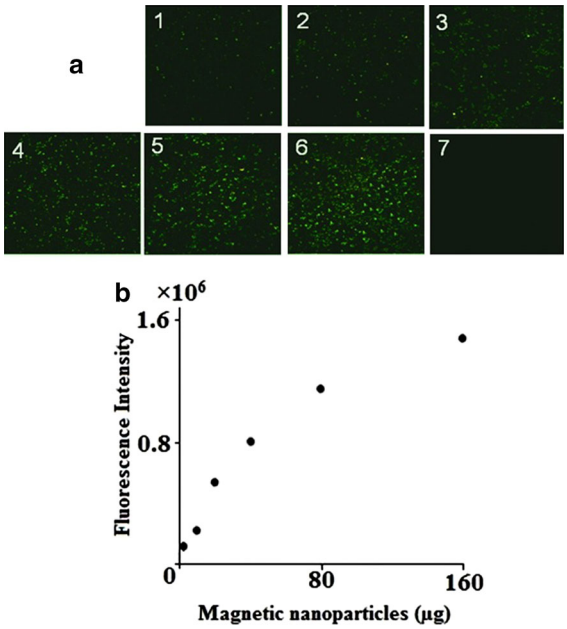

Fig. 3 Fluorescence micrographs of Fe_3O_4@SiO_2 MNPs labeled with dansylcadaverine. **a** Micrographs (a1–a6) represent fluorescence images obtained from 5, 10, 20, 40, 80, and 160 μg of dansylcadaverine labeled Fe_3O_4 @SiO_2 MNPs. The control sample (a7, 20 μg) was prepared by reacting the hydrolyzed NHS ester-coated Fe_3O_4 @SiO_2 MNPs with dansylcadaverine. The fluorescence intensity in a7 is below detection limit. (*Note* the brightness of fluorescence images were adjusted for visual clarity). The original images of (**a**) were processed by a program developed in our lab (supporting information), and the integrated fluorescence intensities of the original images were plotted against quantities of MNPs in (**b**)

same conditions, and no fluorescence signal was detected (data not shown). The quantity of dansylcadaverine conjugated to NHS ester-coated Fe_3O_4@SiO_2 MNPs can be calculated from the fluorescence microscope images. Even though similar fluorescence image-processing software programs were reported in the literature (Fekkar et al. 1998; Rasband 1997–2014), the fluorescence image-processing program employed in this study was developed independently and run in MATLAB environment (Fig. S5, Supporting Information). It is quite clear from Fig. 3 that the fluorescence intensities increased with the increasing amount of dansylcadaverine-coated Fe_3O_4@SiO_2 MNPs (Fig. 3a1–a6). In a control experiment to prove that the fluorophore molecules were immobilized onto the MNPs surface only through covalent attachment, the NHS groups on the surface of Fe_3O_4@SiO_2 MNPs were first hydrolyzed by incubation, then the carboxylic acid-coated Fe_3O_4@SiO_2 MNPs (product of NHS ester hydrolysis) were treated with dansylcadaverine, followed by fluorescence microscopy examination of the extensively washed MNPs. No detectable fluorescence was observed (Fig. 3a7) for such hydrolyzed MNPs incubated with dansylcadaverine, and this result indicated that the nonspecific adsorption of fluorophore to the surface of Fe_3O_4@SiO_2 MNPs was minimal.

Even though the fluorescence microscopic detection of dansylcadaverine-coated Fe_3O_4@SiO_2 MNPs was not quantitative under the conditions employed in our experiment, it was still semi-quantitative as the approach revealed the trend of elevated fluorescence intensities with the increasing amount of fluorophore-coated MNPs. Moreover, the highly sensitive fluorescence microscopy approach allowed for detection of the fluorescence signal from 5 μg of dansylcadaverine-coated Fe_3O_4@SiO_2 MNPs. Compared to the HPLC approach mentioned in "Conjugation of dansylcadaverine to NHS ester-modified Fe_3O4@SiO_2 MNPs" section for accurate measurement of the amount NHS ester groups on Fe_3O_4@SiO_2 MNPs surface, the fluorescence microscopy approach is more convenient for monitoring the incorporation of NHS ester group on nanoparticle surface. The presence of NHS ester on Fe_3O_4@SiO_2 MNPs surface is essential for the application of this type of magnetic nanoparticle reagent in labeling the exposed lysine residues of native proteins (Patil et al. 2013).

Labeling efficiencies of exposed lysine residues in native protein by NHS ester-conjugated Fe_3O_4@SiO_2 MNPs

Reactions between NHS/sulfo-NHS esters and primary amine groups have been widely applied for protein conjugation (Sapsford et al. 2013). Such conjugation reactions can proceed at room temperature in aqueous environments, which allow for detection of the exposed lysine residues in the native structures of proteins. Compared to the volume required to dissolve small molecule labeling reagents such as sulfo-NHS-SS-biotin, large volume of solvent is required to redisperse equivalent amount of the bulky MNPs labeling reagent, and such requirement on solvent would results in dilution of protein in the reaction system and can reduce the primary amine labeling efficiency. For the same initial amount of BSA (100 μg), a larger quantity of NHS ester-coated

MNPs (7 mg) dissolved in larger volume of the solvent (400 μL PBS), captured a smaller amount of protein (27 μg), compared to a smaller quantity of MNPs in a smaller volume of solvent (3 mg MNPs in 200 μL PBS) that captured 52 μg BSA. If the protein concentration in aqueous solvent was below 0.5 mg/mL, the efficiency of the reaction between the primary amine and the NHS ester groups (conjugated to the MNPs) was dramatically decreased due to the hydrolysis of NHS/sulfo-NHS ester.

To circumvent the above-mentioned issues, we employed a special sample mixing method in labeling the exposed lysine residues of native BSA with NHS ester-coated Fe_3O_4@SiO_2 MNPs (Fig. S7). Instead of simply mixing the NHS ester-coated Fe_3O_4@SiO_2 MNPs with BSA all at once, the MNPs were divided into smaller portions and added to the BSA solution separately. After the first addition of the MNPs, the labeling reaction was allowed to proceed for 30 min followed by the addition of the remaining fresh NHS ester-coated MNPs with an additional 30 min of shaking. The reaction volume was kept minimal in order to maintain the initial high concentration of BSA. The addition of fresh NHS ester-coated Fe_3O_4@SiO_2 MNPs was able to label additional lysine residues that were not labeled in the first step due to hydrolysis of NHS ester groups.

To examine the effect of quantity of MNPs and proteins on labeling efficiency, two types of experiments were designed and performed. The first set of experiments involved mixing the same amount of MNPs with different amounts of BSA, and the second set of experiments were designed to mix the same amounts of BSA with different amounts of MNPs. In both cases, MNPs were mixed with BSA by above-mentioned sample-mixing method, and the unbound BSA was quantified by BCA assay. The amounts of BSA conjugated to MNPs in both the approaches were compared in order to understand the effects on labeling efficiency either by increasing the ratio of MNP/BSA (data points in Fig. 4b) or by increasing the ratio of BSA/MNP (data points in Fig. 4a). First, the quantity of BSA conjugated to the NHS ester-coated Fe_3O_4@SiO_2 MNPs (0.5 mg) increased with the increasing amount of BSA until reaching a maximum at 16 μg of BSA added. Further addition of BSA to the reaction did not result in any increased amount of captured BSA, indicating that 0.5 mg of labeled MNP can bind a maximum of 16 μg of BSA. A similar

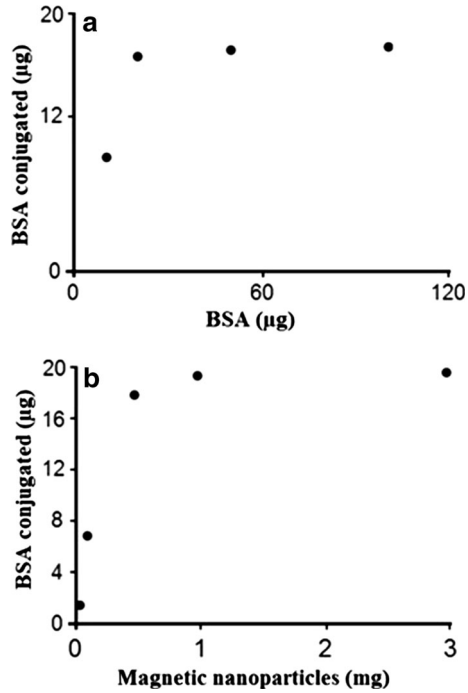

Fig. 4 Quantitative study of labeling BSA by NHS ester-modified Fe_3O_4@SiO_2 MNPs. The amount of BSA conjugated to NHS ester-coated Fe_3O_4@SiO_2 MNPs was calculated by subtracting the amount of remaining BSA from the initial amount of BSA. In the series of experiments presented in Fig. 4a, the amount of NHS ester-coated Fe_3O_4@SiO_2 MNPs (0.5 mg) was kept constant, and the amount of BSA was varied (20, 40, 60, 80, and 100 μg). In Fig. 4b, the quantity of BSA (20 μg) conjugated was kept constant, and the quantity of NHS ester-modified MNPs was varied (0.05, 0.1, 0.5, 1, and 3 mg)

pattern was observed in the second set of experiments, where an increase in the amount of BSA conjugated to Fe_3O_4@SiO_2 MNPs reached to plateau once all the available BSA were labeled. The results from these experiments were in agreement with the constant MNP experiment, with 0.5 mg of labeled MNP binding about 18 μg of protein. The molar ratio of BSA to available NHS ester groups determined by fluorescence experiments was 1:12.

In the first type of experiment (increasing MNP/BSA ratio) when the number of BSA molecules was small, one BSA molecule can be conjugated to a few MNPs. However, as the amount of BSA was increased, several BSA molecules can be conjugated to one magnetic nanoparticle. In the second type of experiment (increasing BSA/MNP ratio), when smaller amounts of MNPs were used, some of the BSA molecules could have multiple sites labeled, and some

might have one site labeled, and some might not be labeled at all; it is also possible that one MNP could label several BSA molecules. As the amount of MNPs increased, the possibility of more lysine residues in one BSA molecule being labeled was increased, but the average number of BSA molecules attached per magnetic nanoparticle could be decreased due to the large number of bulky MNPs present in the system. In case the BSA/MNPs ratio was large, the sample-mixing method described above might not be required as the concentration of BSA was high enough for most of the MNPs to be conjugated by at least one BSA molecule. It is conceivable that the first set of experiments (increasing MNP/BSA ratio) can be done to achieve labeling multiple sites in one protein molecule, and the second set of experiments (increasing BSA/MNP ratio) can be employed to label protein in the way that the native structures of a protein are least disturbed by the labeling.

Conclusion

The reactivity of NHS ester groups conjugated on Fe_3O_4@SiO_2 MNPs surface toward primary amine containing molecules such as the fluorophore dansylcadaverine provides the possibility of qualitative and quantitative characterization of the amount of NHS ester groups immobilized on Fe_3O_4@SiO_2 MNPs surfaces. A disulfide bond in the linker between the fluorophore/NHS ester and Fe_3O_4@SiO_2 MNPs facilitated detachment of the fluorophore from dansycadaverine-modified magnetic MNPs for accurate quantification of NHS ester groups by HPLC analysis. On the other hand, direct measurement of fluorophore-conjugated Fe_3O_4@SiO_2 MNPs with fluorescence microscopy provided a fast and sensitive approach to determine if NHS ester groups were immobilized on the magnetic nanoparticle surface. Maintaining the concentration of fresh NHS ester group in the reaction system is especially important during protein labeling by the bulky NHS ester-coated Fe_3O_4@SiO_2 MNPs, and it can be achieved by adding multiple doses of NHS ester-coated magnetic MNPs to each aliquot of protein during the labeling reaction to increase the labeling efficiency. Such precaution of maintaining the concentration of fresh NHS ester group may not be necessary when trying to label minimum sites in a protein of high concentration, but it is critical to the achievement of labeling as many sites as possible in a protein with multiple sites or protein mixtures such as a cell surface proteome.

Acknowledgments This research was supported in part by the funding received from The Research Institute for Children, Children's Hospital, New Orleans, NIH P01HL076100 to YC, and the Louisiana Board of Regents (LEQSF(2007-12)-ENH-PKSFI-PRS-04). The authors would like to thank Dr. Abouzar Rahmati for his help with writing a program to calculate the intensity of fluorescence microscopic images. They are grateful to Dr. Willie Zhou and his group members for their help on electron microscopy, to Dr. Sourav Chakraborty for the fruitful discussion about microscopic fluorescence measurements, and to Dr. Shiva Adireddy for his guidance with nanoparticles preparation.

References

Bravo-Osuna I, Teutonico D, Arpicco S, Vauthier C, Ponchel G (2007) Characterization of chitosan thiolation and application to thiol quantification onto nanoparticle surface. Int J Pharm 340:173–181. doi:10.1016/j.ijpharm.2007.03.019

Bruce IJ, Sen T (2005) Surface modification of magnetic nanoparticles with alkoxysilanes and their application in magnetic bioseparations. Langmuir 21:7029–7035. doi:10.1021/la050553t

Cannas C et al (2010) $CoFe_2O_4$ and $CoFe_2O_4$/SiO_2 core/shell nanoparticles: magnetic and spectroscopic study. Chem Mater 22:3353–3361. doi:10.1021/cm903837g

Chen Y, Zhang Y (2011) Fluorescent quantification of amino groups on silica nanoparticle surfaces. Anal Bioanal Chem 399:2503–2509. doi:10.1007/s00216-010-4622-7

Chen Y, Chi Y, Wen H, Lu Z (2006) Sensitized luminescent terbium nanoparticles: preparation and time-resolved fluorescence assay for DNA. Anal Chem 79:960–965. doi:10.1021/ac061477h

Chiriaco F, Soloperto G, Greco A, Conversano F, Ragusa A, Menichetti L, Casciaro S (2013) Magnetically-coated silica nanospheres for dual-mode imaging at low ultrasound frequency. World J Radiol 5:411–420. doi:10.4329/wjr.v5.i11.411

Corsi K, Chellat F, Yahia LH, Fernandes JC (2003) Mesenchymal stem cells, MG63 and HEK293 transfection using chitosan-DNA nanoparticles. Biomaterials 24:1255–1264. doi:10.1016/S0142-9612(02)00507-0

Coussot G, Nicol E, Commeyras A, Desvignes I, Pascal R, Vandenabeele-Trambouze O (2009) Colorimetric quantification of amino groups in linear and dendritic structures. Polym Int 58:511–518. doi:10.1002/pi.2560

Dauginet L, Duwez AS, Legras R, Demoustier-Champagne S (2001) Surface Modification of Polycarbonate and Poly (ethylene terephthalate) Films and Membranes by Polyelectrolyte Deposition. Langmuir 17:3952–3957. doi:10.1021/la001333c

Dementev N, Feng X, Borguet E (2009) Fluorescence labeling and quantification of oxygen-containing functionalities on

the surface of single-walled carbon nanotubes. Langmuir 25:7573–7577. doi:10.1021/la803947q

Elzey S, Tsai DH, Rabb SA, Yu LL, Winchester MR, Hackley VA (2012) Quantification of ligand packing density on gold nanoparticles using ICP-OES. Anal Bioanal Chem 403:145–149. doi:10.1007/s00216-012-5830-0

Fang C, Bhattarai N, Sun C, Zhang M (2009) Functionalized nanoparticles with long-term stability in biological media. Small 5:1637–1641. doi:10.1002/smll.200801647

Fekkar H, Benbernou N, Esnault S, Shin HC, Guenounou M (1998) Multiparameter fluorescence imaging for quantification of TH-1 and TH-2 cytokines at the single-cell level. Proceedings of SPIE, Optical investigations of cells in vitro and in vivo, vol 3260, pp 96–104. doi:10.1117/12.307108

Feng X, Dementev N, Feng W, Vidic R, Borguet E (2006) Detection of low concentration oxygen containing functional groups on activated carbon fiber surfaces through fluorescent labeling. Carbon 44:1203–1209. doi:10.1016/j.carbon.2005.10.057

Ghasemi M, Minier M, Tatoulian M, Arefi-Khonsari F (2007) Determination of amine and aldehyde surface densities: application to the study of aged plasma treated polyethylene films. Langmuir 23:11554–11561. doi:10.1021/la701126t

Gupta AK, Gupta M (2005) Synthesis and surface engineering of iron oxide nanoparticles for biomedical applications. Biomaterials 26:3995–4021. doi:10.1016/j.biomaterials.2004.10.012

He J, Huang M, Wang D, Zhang Z, Li G (2014) Magnetic separation techniques in sample preparation for biological analysis: a review. J Pharm Biomed Anal. doi:10.1016/j.jpba.2014.04.017

Hinterwirth H, Kappel S, Waitz T, Prohaska T, Lindner W, Lammerhofer M (2013) Quantifying thiol ligand density of self-assembled monolayers on gold nanoparticles by inductively coupled plasma-mass spectrometry. ACS Nano 7:1129–1136. doi:10.1021/nn306024a

Ikari A, Takiguchi A, Atomi K, Sugatani J (2011) Epidermal growth factor increases clathrin-dependent endocytosis and degradation of claudin-2 protein in MDCK II cells. J Cell Physiol 226:2448–2456. doi:10.1002/jcp.22590

Kell AJ, Simard B (2007) Vancomycin architecture dependence on the capture efficiency of antibody-modified microbeads by magnetic nanoparticles. Chem Commun 12:1227–1229. doi:10.1039/B617427B

Kim J, Shon HK, Jung D, Moon DW, Han SY, Lee TG (2005) Quantitative chemical derivatization technique in time-of-flight secondary ion mass spectrometry for surface amine groups on plasma-polymerized ethylenediamine film. Anal Chem 77:4137–4141. doi:10.1021/ac0500683

Kim J, Jung D, Park Y, Kim Y, Moon DW, Lee TG (2007) Quantitative analysis of surface amine groups on plasma-polymerized ethylenediamine films using UV–visible spectroscopy compared to chemical derivatization with FT-IR spectroscopy, XPS and TOF-SIMS. Appl Surf Sci 253:4112–4118. doi:10.1016/j.apsusc.2006.09.011

Kolhatkar AG, Jamison AC, Litvinov D, Willson RC, Lee TR (2013) Tuning the magnetic properties of nanoparticles. Int J Mol Sci 14:15977–16009. doi:10.3390/ijms140815977

Larumbe S, Gomez-Polo C, Perez-Landazabal JI, Pastor JM (2012) Effect of a SiO_2 coating on the magnetic properties of Fe_3O_4 nanoparticles. J Phys Condens Matter Inst Phys J 24:266007. doi:10.1088/0953-8984/24/26/266007

Liu Y, Yan B (2011) Characterizing the surface chemistry of nanoparticles: an analogy to solid-phase synthesis samples. Comb Chem High Throughput Screen 14:191–197

Liu WB, Yang BJ, Yang WL, Li W, Yang J, Gao MZ (2013) Synthesis of magnetic particles and silica coated core-shell materials. Adv Mater Res 631–632:490–493. doi:10.4028/www.scientific.net/AMR.631-632.490

Lu Y, Yin Y, Mayers BT, Xia Y (2002) Modifying the surface properties of superparamagnetic iron oxide nanoparticles through a sol—gel approach. Nano Lett 2:183–186. doi:10.1021/nl015681q

Malvindi MA et al (2011) Magnetic/silica nanocomposites as dual-mode contrast agents for combined magnetic resonance imaging and ultrasonography. Adv Funct Mater 21:2548–2555. doi:10.1002/adfm.201100031

MATLAB and statistics toolbox release R2013a TM. The MathWorks, Inc., Natick

Maus L, Spatz JP, Fiammengo R (2009) Quantification and reactivity of functional groups in the ligand shell of PEGylated gold nanoparticles via a fluorescence-based assay. Langmuir 25:7910–7917. doi:10.1021/la900545t

Noel S, Liberelle B, Robitaille L, De Crescenzo G (2011) Quantification of primary amine groups available for subsequent biofunctionalization of polymer surfaces. Bioconjug Chem 22:1690–1699. doi:10.1021/bc200259c

Patil US, Qu H, Caruntu D, O'Connor CJ, Sharma A, Cai Y, Tarr MA (2013) Labeling primary amine Groups in peptides and proteins with N-hydroxysuccinimidyl ester modified Fe_3O_4@SiO_2 nanoparticles containing cleavable disulfide-bond linkers. Bioconjug Chem 24:1562–1569. doi:10.1021/bc400165r

Pellenbarg T, Dementev N, Jean-Gilles R, Bessel C, Borguet E, Dollahon N, Giuliano R (2010) Detecting and quantifying oxygen functional groups on graphite nanofibers by fluorescence labeling of surface species. Carbon 48:4256–4267. doi:10.1016/j.carbon.2010.07.035

Rasband WS (1997–2014) ImageJ, U. S. National Institutes of Health, Bethesda, Maryland, USA. http://imagej.nih.gov/ij/

Sapsford KE et al (2013) Functionalizing nanoparticles with biological molecules: developing chemistries that facilitate nanotechnology. Chem Rev 113:1904–2074. doi:10.1021/cr300143v

Schellenberger EA, Sosnovik D, Weissleder R, Josephson L (2004) Magneto/optical annexin V, a multimodal protein. Bioconjug Chem 15:1062–1067. doi:10.1021/bc049905i

Simon M, Sze KKN (1981) Physics of semiconductor devices, 1st edn. Wiley, New York

Sun Q, Yan B (1998) Single bead IR monitoring of a novel benzimidazole synthesis. Bioorg Med Chem Lett 8:361–364

Turcheniuk K, Tarasevych AV, Kukhar VP, Boukherroub R, Szunerits S (2013) Recent advances in surface chemistry strategies for the fabrication of functional iron oxide based magnetic nanoparticles. Nanoscale 5:10729–10752. doi:10.1039/C3NR04131J

Urbanova V, Magro M, Gedanken A, Baratella D, Vianello F, Zboril R (2014) Nanocrystalline iron oxides, composites, and related materials as a platform for electrochemical,

magnetic, and chemical biosensors. Chem Mater 26:6653–6673. doi:10.1021/cm500364x

van de Waterbeemd M, Sen T, Biagini S, Bruce IJ (2010) Surface functionalisation of magnetic nanoparticles: quantification of surface to bulk amine density. Micro Nano Lett IET 5:282–285. doi:10.1049/mnl.2010.0112

Vaughan JC, Dempsey GT, Sun E, Zhuang X (2013) Phosphine quenching of cyanine dyes as a versatile tool for fluorescence microscopy. J Am Chem Soc 135:1197–1200. doi:10.1021/ja3105279

Verma A, Stellacci F (2010) Effect of surface properties on nanoparticle–cell interactions. Small (Weinh Bergstr Ger) 6:12–21. doi:10.1002/smll.200901158

Villanueva A et al (2009) The influence of surface functionalization on the enhanced internalization of magnetic nanoparticles in cancer cells. Nanotechnology 20:115103/115101–115103/115109. doi:10.1088/0957-4484/20/11/115103

Xing Y, Borguet E (2006) Specificity and sensitivity of fluorescence labeling of surface species. Langmuir 23:684–688. doi:10.1021/la060994s

Xing Y, Dementev N, Borguet E (2007) Chemical labeling for quantitative characterization of surface chemistry. Curr Opin Solid State Mater Sci 11:86–91. doi:10.1016/j.cossms.2008.07.002

Yan B et al (2013) Characterization of surface ligands on functionalized magnetic nanoparticles using laser desorption/ionization mass spectrometry (LDI-MS). Nanoscale 5:5063–5066. doi:10.1039/C3NR01384G

Yu WW, Falkner JC, Yavuz CT, Colvin VL (2004) Synthesis of monodisperse iron oxide nanocrystals by thermal decomposition of iron carboxylate salts. Chem Commun 20:2306–2307. doi:10.1039/B409601K

Zhang Y, Chen Y (2012) Fmoc-Cl fluorescent determination for amino groups of nanomaterial science. IET Nanobiotechnol 6:76–80. doi:10.1049/iet-nbt.2011.0027

Zhou H, Li X, Lemoff A, Zhang B, Yan B (2010) Structural confirmation and quantification of individual ligands from the surface of multi-functionalized gold nanoparticles. Analyst 135:1210–1213. doi:10.1039/C0AN00066C